ELSEVIER

European Journal of Pharmacology 393 (2000) 123–135

ejp

www.elsevier.nl/locate/ejphar

Pharmacological and null mutation approaches reveal nicotinic receptor diversity

Paul Whiteaker [a,*], Michael J. Marks [a], Sharon R. Grady [a], Ying Lu [a], Marina R. Picciotto [b], Jean-Pierre Changeux [c], Allan C. Collins [a]

[a] *Institute for Behavioral Genetics, University of Colorado, Campus Box 447, Boulder, CO 80303-0447, USA*
[b] *Department of Psychiatry, Yale University School of Medicine, New Haven, CT, USA*
[c] *Laboratory of Molecular Neurobiology, Institute Pasteur, Paris, France*

Accepted 21 January 2000

Abstract

We have developed an array of assays for nicotinic acetylcholine receptor binding and function. [^{125}I]α-Bungarotoxin-, (−)-[^{3}H]nicotine-, and [^{3}H]epibatidine-binding nicotinic acetylcholine receptors were assayed in mouse brain membranes and sections. Nicotinic acetylcholine receptor function was quantified using synaptosomal [^{3}H]dopamine, [^{3}H]γ-aminobutyric acid ([^{3}H]GABA), and $^{86}Rb^{+}$ efflux techniques. Additionally, the effects of β2 subunit deletion on each of the measures were assessed. Detailed pharmacological comparison revealed minimally six nicotinic binding subtypes: [^{125}I]α-bungarotoxin-binding nicotinic acetylcholine receptors; β2-subunit-dependent and -independent high-affinity (−)-[^{3}H]nicotine-binding sites; β2-dependent and -independent cytisine-resistant [^{3}H]epibatidine-binding sites; and a β2-dependent low-affinity [^{3}H]epibatidine binding site. Comparative pharmacology suggested that [^{3}H]GABA and dihydro-β-erythroidine (DHβE)-sensitive $^{86}Rb^{+}$ efflux are mediated by the same (probably α4β2) nicotinic acetylcholine receptor subtype, while other nicotinic acetylcholine receptor subtypes evoke [^{3}H]dopamine and DHβE-resistant $^{86}Rb^{+}$ efflux. In whole-brain preparations, each measure of nicotinic acetylcholine receptor function was β2 dependent. The majority of β2-independent [^{3}H]epibatidine binding was located in small, scattered brain nuclei, suggesting that individual nuclei may prove suitable for identification of novel, native nicotinic acetylcholine receptors.

Keywords: Nicotinic acetylcholine receptor; Pharmacological comparison; Subunit null mutation; Binding; Activation

1. Introduction

Molecular cloning techniques have identified nine nicotinic acetylcholine receptor subunits (α2–7, β2–4), the mRNAs of which are expressed in varying patterns and quantities throughout the mammalian brain (Lindstrom et al., 1996). Mature nicotinic acetylcholine receptors appear to be pentameric assemblies of these subunits, and because different combinations of subunits produce receptors of different subtypes, the potential for nicotinic acetylcholine receptor diversity in mammalian brain is vast.

Identifying which nicotinic acetylcholine receptor subtypes are expressed in mammalian central nervous system (CNS) has been a difficult task due to a paucity both of truly subtype specific nicotinic compounds, and of well-characterized assays for nicotinic receptor binding and activation. These problems exacerbate each other, and progress in one area is likely to have positive repercussions in the other. To date, extensive biochemical data have only been collected for two native nicotinic acetylcholine receptor subtypes: the ''high-affinity agonist binding'' α4β2 subtype (labeled by [^{3}H]cytisine and (−)-[^{3}H]nicotine; Whiting and Lindstrom, 1987; Flores et al., 1992; Picciotto et al., 1995; Marubio et al., 1998) and the predominantly or entirely α7 subtype (labeled by [^{125}I]α-bungarotoxin, Schoepfer et al., 1990; Seguela et al., 1992). Identification of additional naturally expressed nicotinic acetylcholine receptor subtypes is a priority as it will yield insights into the rules governing assembly of subunit peptides into receptor proteins, facilitate generation and isola-

* Corresponding author. Tel.: +1-303-492-8752; fax: +1-303-492-8063.

0014-2999/00/$ - see front matter
PII: S0014-2999(00)00052-2

tion of subtype specific compounds, and enhance understanding of the physiological roles of individual neuronal nicotinic acetylcholine receptor subtypes in normal and/or pathological states.

One of our laboratory's main priorities has been to develop and characterize binding and functional assays of nicotinic receptors. The primary motivation in this effort has been to identify discrepancies between different measures of nicotinic acetylcholine receptor binding and function, which would indicate heterogeneity in the nicotinic acetylcholine receptor populations responsible.

[^{3}H]Epibatidine has been shown to bind to multiple nicotinic acetylcholine receptor subtypes with high-affinity (Perry and Kellar, 1995; Marks et al., 1998; Parker et al., 1998). In rat (Perry and Kellar, 1995) and mouse (Marks et al., 1998) CNS, the majority of high-affinity [^{3}H]epibatidine binding occurs at the $\alpha 4\beta 2$ subtype nicotinic acetylcholine receptor, but additional sites (distinguished by their relatively low cytisine affinity) are also expressed in small nuclei, dispersed across the brain. This information provided the impetus to use [^{3}H]epibatidine binding as a tool to identify novel nicotinic acetylcholine receptor subtypes in mouse brain.

A growing consensus that many nicotinic acetylcholine receptors are located presynaptically, where they modulate neurotransmitter release (Wonnacott, 1997), has encouraged efforts to study nicotinic acetylcholine receptor function in preparations of isolated nerve termini, or synaptosomes. Accordingly, we have concentrated our efforts on developing novel functional assays of nicotinic acetylcholine receptor mediated synaptosomal release. Such assays may be divided into those that monitor neurotransmitter release, an indirect measure of nicotinic acetylcholine receptor activation, and those that measure ion flux through the nicotinic acetylcholine receptor directly. In the first category, we have described nicotinic acetylcholine receptor-mediated mouse brain synaptosomal [^{3}H]dopamine (Grady et al., 1992) and [^{3}H]γ-aminobutyric acid ([^{3}H]GABA) (Lu et al., 1998) efflux assays. In order to directly measure nicotinic acetylcholine receptor-mediated ion flux, we have characterized $^{86}Rb^+$ efflux assays, using both discrete sampling (Marks et al., 1993) and continuous flow monitoring detection, which offers considerable increases in temporal resolution (Marks et al., 1999). Ion flux assays offer a means to measure activation of all of the nicotinic acetylcholine receptors in a given preparation, while neurotransmitter release assays will only measure activation of nicotinic acetylcholine receptors associated with synaptosomes containing the transmitter in question. Whether this added selectivity is an advantage depends on the particular experimental application. Detailed pharmacological comparisons among these biochemical assays indicate considerable heterogeneity in the nicotinic acetylcholine receptor-mediated responses, suggesting mediation by a number of different nicotinic acetylcholine receptor subtypes.

As an adjunct to the conventional pharmacological approach, we have begun to use subunit null mutant animals, as a further tool to provide insights as to the identities of these putative nicotinic acetylcholine receptor subtypes. Changes in, or losses of, nicotinic measures upon alterations in nicotinic acetylcholine receptor subunit gene expression powerfully implicate that gene's product as a component of the nicotinic acetylcholine receptor mediating the tested measure. The results reported here demonstrate the utility of $\beta 2$-null mutant mice in establishing the role of the $\beta 2$ nicotinic acetylcholine receptor subunit in binding and functional measures of mouse brain nicotinic acetylcholine receptors.

2. Materials and methods

2.1. Materials

[7,8-^{3}H]Dopamine (40–60 Ci/mmol), (−)-[*N*-methyl-^{3}H]nicotine (75 Ci/mmol), [^{125}I]α-bungarotoxin (initial specific activity 200 Ci/mmol) and [^{3}H]GABA (84–90 Ci/mmol) were obtained from Amersham, Arlington Heights, IL. [^{3}H]Epibatidine (33.8 Ci/mmol), and carrier free ^{86}RbCl were bought from DuPont-NEN, Boston, MA. The following compounds were purchased from Research Biochemicals International, Natick, MA: (+)-epibatidine hydrochloride, (−)-epibatidine hydrochloride, (+)-anatoxin-a, epiboxidine, dihydro-β-erythroidine (DHβE) and 3-(2-(*S*)-azetidinylmethoxy)pyridine dihydrochloride (A85380). Sucrose and HEPES hemisodium salt were bought from Boehringer-Mannheim (Indianapolis, IN). Econosafe scintillation cocktail was a product of Research Products International, Arlington Heights, IL. Mecamylamine was a gift from Merck Sharp and Dohme Research Laboratory, Rahway, NJ. All other chemicals were sourced from Sigma, St. Louis, MO.

2.2. Mice

C57BL/6J and $\beta 2$ nicotinic acetylcholine receptor null mutant mice (Picciotto et al., 1995) were bred at the Institute for Behavioral Genetics (University of Colorado, Boulder, CO). C57BL/6J mice were housed five per cage, and $\beta 2$ nicotinic acetylcholine receptor null mutant mice were housed with like-sex littermates (two to five per cage). Mice were maintained in a vivarium at 22°C with a 12-h light/dark cycle (lights on from 7 AM to 7 PM). The mice were allowed free access to food (Harlan Tekland Rodent Diet) and water. Animals of both sexes were used between 60 and 90 days of age. All animal care and experimental procedures were performed in accordance with the guidelines and with the approval of the Animal Care and Utilization Committee of the University of Colorado, Boulder.

2.3. Autoradiography: preparation of sections

Autoradiography procedures were similar to those described previously (Pauly et al., 1989; Marks et al., 1998). Mice (C57BL/6J or wild-type, heterozygous, or homozygous β2-null mutants) were killed by cervical dislocation, the brains were removed from the skull and rapidly frozen by immersion in isopentane (−35°C, 10 s). The frozen brains were wrapped in aluminum foil, packed in ice, and stored at −70°C until sectioning. Tissue sections (14 μm thick) prepared using an IEC Minotome Cryostat refrigerated to −16°C were thaw-mounted onto subbed microscope slides (Richard Allen, Richland, MI). Slides were subbed by incubation with gelatin (1% w/v)/chromium aluminum sulfate (0.1% w/v) for 2 min at 37°C, drying overnight at 37°C, incubation at 37°C for 30 min in 0.1% (w/v) poly-L-lysine in 25 mM Tris (pH = 8.0), and drying at 37°C overnight. Mounted sections were stored, desiccated, at −70°C until use. Between 6 and 10 series of sections were collected from each mouse brain.

2.4. Autoradiography: (−)-[^{3}H]nicotine binding

Series of mouse brain sections were incubated in binding buffer (NaCl, 144 mM; KCl, 1.5 mM; $CaCl_2$, 2 mM; $MgSO_4$, 1 mM; HEPES, 20 mM; pH = 7.5) at 22°C for 10 min, prior to (−)-[^{3}H]nicotine binding. The samples were then incubated with 20 nM (−)-[^{3}H]nicotine for 1 h at 22°C. An adjacent series of sections from each mouse was used to determine non-specific (−)-[^{3}H]nicotine binding (in the presence of 1 mM (−)-nicotine bitartrate). The slides were then washed as follows (all washes at 0°C): 5 s in binding buffer (twice), 5 s in 0.1× binding buffer (twice), 5 s in 5 mM HEPES (pH = 7.5), twice.

2.5. Autoradiography: [^{125}I]α-bungarotoxin binding

A series of sections from each mouse was incubated in binding buffer +0.1% (w/v) bovine serum albumin at 22°C for 10 min. The samples were then incubated with 2 nM [^{125}I]α-bungarotoxin in binding buffer +0.1% (w/v) bovine serum albumin for 4 h at 22°C. An adjacent series of sections from each mouse was used to determine non-specific [^{125}I]α-bungarotoxin binding (in the presence of 1 mM (−)-nicotine bitartrate). The slides were then washed as follows (all washes at 0°C): 10 min in binding buffer (twice), 5 s in 0.1× binding buffer (twice), 5 s in 5 mM HEPES (pH = 7.5), twice.

2.6. Autoradiography: high-affinity [^{3}H]epibatidine binding

Sections for use in [^{3}H]epibatidine binding were incubated in binding buffer at 22°C for 10 min, followed by incubation with 500 pM [^{3}H]epibatidine for 2 h at 22°C. Three series of adjacent sections were used from each mouse to measure total [^{3}H]epibatidine binding (no competing ligand), [^{3}H]epibatidine binding in the presence of 50 nM unlabeled cytisine (cytisine-resistant binding), and non-specific [^{3}H]epibatidine binding (in the presence of 1 mM unlabeled (−)-nicotine). The concentration of unlabeled cytisine was chosen on the basis of results obtained by Marks et al. (1998). Slides were washed by sequential incubation in the following buffers (all steps at 0°C): 5 s in binding buffer (twice), 5 s in 0.1× binding buffer (twice), and twice for 5 s in 5 mM HEPES (pH = 7.5).

2.7. Autoradiography: image collection

Labeled sections were initially dried with a stream of air, then by overnight storage (22°C) under vacuum. Mounted, desiccated sections were apposed to film (4–7 days, Amersham Hyperfilm β-Max film for [^{125}I]α-bungarotoxin-labeled sections; 8–12 weeks, Amersham Hyperfilm-^{3}H for ^{3}H-labeled sections). After the films had been exposed to the sections for an appropriate length of time, they were developed, the films were illuminated using a Northern Light light box, and autoradiographic images of the sections were captured using a CCD imager camera.

2.8. Membrane preparation

Each mouse (C57BL/6J or wild-type, heterozygous, or homozygous β2-null mutant) was killed by cervical dislocation. The brain was removed from the skull and placed on an ice-cold platform. The hindbrain, cerebellum and olfactory bulbs were discarded without further dissection (''whole-brain'' preparation). Samples were homogenized in ice-cold hypotonic buffer (NaCl, 14.4 mM; KCl, 0.2 mM; $CaCl_2$, 0.2 mM; $MgSO_4$, 0.1 mM; HEPES 2 mM; pH = 7.5) using a Teflon-glass tissue grinder. The particulate fractions were obtained by centrifugation at 20000 × *g* (15 min, 4°C; Sorval RC-2B centrifuge). The pellets were resuspended in fresh homogenization buffer, incubated at 22°C for 10 min, then harvested by centrifugation as before. Each pellet was washed twice more by resuspension/centrifugation, then stored (in pellet form under homogenization buffer) at −70°C until used. Protein concentrations in the membrane preparations were measured according to the method of Lowry et al. (1951), using bovine serum albumin as the standard.

2.9. Ligand binding to membranes

High-affinity [^{3}H]epibatidine binding (at low ligand concentrations) was quantified as described previously (Marks et al., 1998). Incubations were performed in 1-ml polypropylene tubes in a 96-well format, using 200 μg of whole-brain membrane protein per tube. A 500-μl reaction volume was used to minimize problems of ligand depletion, and all incubations progressed for 2 h at 22°C. The

concentration of [^{3}H]epibatidine (500 pM) used in inhibition binding experiments was chosen to maintain binding of ligand to the tissue at 5% or less of total ligand added. Cytisine-resistant [^{3}H]epibatidine binding was determined by including 50 nM cytisine in the incubation conditions. Non-specific binding was determined in all experiments by the addition of 1 mM (−)-nicotine. Filter counts were determined by liquid scintillation counting.

Binding of [^{3}H]epibatidine at high ligand concentrations (low plus high-affinity binding) was measured as described by Marks et al. (1999), using a 100-μl incubation volume. Total [^{3}H]epibatidine binding was determined in the presence of 10 nM [^{3}H]epibatidine at 22°C for 60 min. Non-specific binding was measured by the inclusion of 1 mM (−)-nicotine in the incubation. Low-affinity binding was calculated by subtracting [^{3}H]epibatidine binding at 500 pM from that measured at 10-nM-labeled ligand, or as the amount of low-affinity binding inhibited by incubation with 300 μM dTC.

Total (−)-[^{3}H]nicotine binding to membrane preparations was performed using the same protocol as for high concentration (low + high affinity) [^{3}H]epibatidine binding, but samples were incubated with (−)-[^{3}H]nicotine (20 nM) at 22°C for 30 min.

2.10. Synaptosome preparation

Mice (C57BL/6J or wild-type, heterozygous, or homozygous β2-null mutants) were killed by cervical dislocation. Brains were removed from the skulls and placed on an ice-cold platform. For $^{86}Rb^+$ and [^{3}H]GABA release experiments the hindbrain, cerebellum and olfactory bulbs were discarded without further dissection, resulting in a ''whole-brain'' tissue sample. Striatal tissue alone was collected for use in [^{3}H]dopamine release experiments. Tissue was resuspended in 10 volumes of isotonic sucrose solution (0.32 M sucrose, 5 mM HEPES, pH = 7.5). Crude synaptosomal preparations were made by homogenization in a hand-held glass/PTFE tissue grinder (20 strokes). The homogenate was centrifuged at $500 \times g$ for 10 min, and the resulting supernatant was then centrifuged at $12{,}000 \times g$ for 20 min to yield the synaptosomal P2 pellet.

2.11. $^{86}Rb^+$ superfusion protocol (continuous flow monitoring, fraction collection)

$^{86}Rb^+$ efflux superfusion using continuous flow monitoring was performed according to the protocol of Marks et al. (1999). Synaptosomal P2 pellets were resuspended into uptake buffer (NaCl, 140 mM; KCl, 1.5 mM; $CaCl_2$, 2 mM; $MgSO_4$, 1 mM; HEPES hemisodium salt 25 mM; glucose 20 mM; pH = 7.5) and then loaded with $^{86}Rb^+$. Loading was achieved by incubation with 4 μCi of carrier free $^{86}Rb^+$ at 22°C for 30 min in a final volume of 35 μl. Samples to be used with acetylcholine were incubated during loading with diisopropylfluorophosphate (10 μM), an irreversible inhibitor of cholinesterase, for the least 10 min of loading. Uptake was terminated and unincorporated $^{86}Rb^+$ removed by filtration of the sample under gentle vacuum (−0.2 atm) onto a 6-mm-diameter glass fiber filter (Type A/E; Gelman, Ann Arbor, MI), followed by two washes with 0.5 ml uptake buffer.

Following filtration and wash, glass fiber filters containing $^{86}Rb^+$ loaded synaptosomes were transferred to polypropylene superfusion supports. $^{86}Rb^+$ perfusion buffer (NaCl, 135 mM; CsCl, 5 mM; KCl, 1.5 mM; $CaCl_2$, 2 mM; $MgSO_4$, 1 mM; HEPES hemisodium salt 25 mM; glucose 20 mM; tetrodotoxin 50 nM; bovine serum albumin (fraction V), 0.1%; pH = 7.5) was delivered to the filters at the rate of 2.5 ml/min using a peristaltic pump (Gilson Minpuls 3; Gilson, Middleton, WI). Buffer was removed from the platforms at using a pump running at a higher rate (3.2 ml/min), preventing the accumulation of perfusion buffer on top of the filters. Efflux of $^{86}Rb^+$ from the samples was achieved by pumping the superfusate through a 200-μl volume flow-through Cherenkov counting cell in a β-RAM radioactivity high-pressure liquid chromatography detector (IN/US systems, Tampa, FL). Stimulation of the samples was performed by diverting perfusion buffer through a 200-μl test loop containing the test solution by means of a four-way PTFE injection valve (Alltech associates, Deerfield, IL), producing a stimulation time of 5 s. DHβE-sensitive $^{86}Rb^+$ efflux was measured following stimulation with 10 μM (−)-nicotine, while DHβE-resistant $^{86}Rb^+$ efflux was evoked using 10 μM epibatidine + 2 μM DHβE (present throughout the superfusion process where used). When samples were to be stimulated with acetylcholine or carbachol, the perfusion buffer was supplemented with atropine (1 μM). Each synaptosomal sample was stimulated only once, and release of $^{86}Rb^+$ from the samples was monitored for a total of 4 min, with the stimulating pulse arriving at 2 min. This timing permitted the definition of basal efflux before and after agonist application.

Where $^{86}Rb^+$ efflux was monitored by fraction collection, the procedures were identical to those described above with the following modifications: buffer perfusion rate was 2 ml/min, buffer was removed using a pump running at a higher rate (2.5 ml/min), fractions of eluate were collected every 30 s, and their radioactive contents were assessed using a Packard Tricarb 1600 gamma counter.

2.12. [^{3}H]Dopamine superfusion protocol

[^{3}H]Dopamine superfusion was performed using a modification of the protocol of Grady et al. (1997). The P2 synaptosomal pellet was resuspended into 800 μl of dopamine perfusion buffer (NaCl, 128 mM; KCl, 2.4 mM;

$CaCl_2$, 3.2 mM; KH_2PO_4, 1.2 mM; $MgSO_4$, 1.2 mM; HEPES hemisodium salt 25 mM; glucose 10 mM; ascorbic acid, 1 mM; pargyline, 10 μM; pH = 7.5), and incubated at 37°C for 10 min. [^{3}H]Dopamine was added (4 μCi, yielding a final concentration of approximately 0.1 μM), and incubation was continued for a further 5 min. Samples to be used with acetylcholine were incubated during loading with diisopropylfluorophosphate (10 μM), an irreversible inhibitor of cholinesterase. Samples (80 μl) were collected and loading terminated by collection onto 6-mm-diameter glass fiber filters and washing with superfusion buffer, as for $^{86}Rb^+$-loaded synaptosomes.

Washed filters bearing loaded synaptosomes were transferred onto 13-mm Gelman type A/E filters on polypropylene platforms, and perfused with buffer (dopamine perfusion buffer supplemented with 10 μM nomifensine and 0.1% w/v bovine serum albumin; atropine (1 μM) was added when samples were to be stimulated with acetylcholine or carbachol) at a rate of 0.6 ml/min for 10 min before fraction collection was started. Fractions were collected every 30 s, and buffer was actively pumped away from the platforms at a rate of 1 ml/min. Agonists and antagonists were added to the perfusion buffer for 30 s (one fraction).

2.13. [^{3}H]GABA superfusion protocol

[^{3}H]GABA superfusion was performed according to the protocol of Lu et al. (1998). Synaptosomal P2 pellets were resuspended into GABA perfusion buffer (NaCl, 128 mM; KCl, 2.4 mM; $CaCl_2$, 3.2 mM; KH_2PO_4, 1.2 mM; $MgSO_4$, 1.2 mM; HEPES hemisodium salt 25 mM; glucose 10 mM; pH = 7.5), then incubated for 10 min at 37°C with 1 mM aminooxyacetic acid (an inhibitor of GABA aminotransferase), prior to [^{3}H]GABA loading. Loading was achieved by incubation for a further 10 min at 37°C in the presence of [^{3}H]GABA and unlabeled GABA (to final concentrations of 0.1 and 0.25 μM, respectively). Samples to be used with acetylcholine were incubated during loading with diisopropylfluorophosphate (10 μM), an irreversible inhibitor of cholinesterase. Loading was terminated by collection of samples onto glass fiber filters and washing with superfusion buffer, as for $^{86}Rb^+$-loaded synaptosomes.

As for [^{3}H]dopamine perfusion experiments, washed filters bearing [^{3}H]GABA-loaded synaptosomes were transferred onto 13-mm Gelman type A/E filters on polypropylene platforms, and perfused with buffer (perfusion buffer supplemented with 0.1% w/v bovine serum albumin; atropine (1 μM) was added when samples were to be stimulated with acetylcholine or carbachol). Buffer was pumped on at a rate of 1.8 ml/min for 10 min before fraction collection was started. Fractions were collected every 12 s, and buffer was actively pumped away from the platforms at a rate of 2.4 ml/min. Agonists and antagonists were added to the perfusion buffer for 12 s (one fraction).

2.14. Data analysis

Agonist stimulated $^{86}Rb^+$, [^{3}H]dopamine and [^{3}H]-GABAefflux were determined as follows. The fractions preceding and following stimulation represent basal release, and were fit as the first-order process $E_t = E_o e^{-kT}$, where E_t is the efflux at time t, E_o is the initial basal efflux, and k is the rate of decline of efflux. This allowed calculation of theoretical basal efflux in each fraction. Agonist stimulated release was then quantified by subtracting theoretical basal release from the number of counts measured during agonist exposure. For $^{86}Rb^+$ efflux, filter counts were assessed at the end of each experiment, and $^{86}Rb^+$ efflux was normalized as percent of tissue $^{86}Rb^+$ contents released by agonist exposure. For [^{3}H]dopamine and [^{3}H]GABA efflux experiments, agonist stimulated release was normalized as a multiple of theoretical baseline release.

Dose–response curves were fitted using either the Michaelis–Menten equation, the Hill equation, or two Michaelis–Menten equations simultaneously. Curve fitting was performed using the nonlinear curve fitting algorithm in SigmaPlot 5.0 (Jandel Scientific, San Rafael, CA).

3. Results

3.1. Autoradiography

The nicotinic ligands (−)-[^{3}H]nicotine, [^{3}H]epibatidine, and [^{125}I]α-bungarotoxin exhibited considerable variation in their binding patterns at the levels of the superior and inferior colliculi, as illustrated in Fig. 1. (−)-[^{3}H]Nicotine binding was widespread at the level of the superior colliculus in wild-type animals. Particularly high densities of (−)-[^{3}H]nicotine binding were seen in the whole of the interpeduncular nucleus, and the superior colliculus. The thalamus and some layers of the cortex were also relatively densely labeled. The pattern of [^{3}H]epibatidine binding closely resembled that of (−)-[^{3}H]nicotine binding, but binding densities in the superficial layers of the superior colliculus and in the interpeduncular nucleus were much greater, making [^{3}H]epibatidine binding in the rest of the section appear fainter by comparison. Cytisine-resistant [^{3}H]epibatidine binding at this level of the brain was restricted to the interpeduncular nucleus and the superficial layers of the superior colliculus, the regions that differed between the (−)-[^{3}H]nicotine and [^{3}H]epibatidine binding patterns. In contrast, the highest levels of [^{125}I]α-bungarotoxin binding were seen in the outer shell of the interpeduncular nucleus, the superficial layers of the superior colliculus, the subiculum, and the red nucleus.

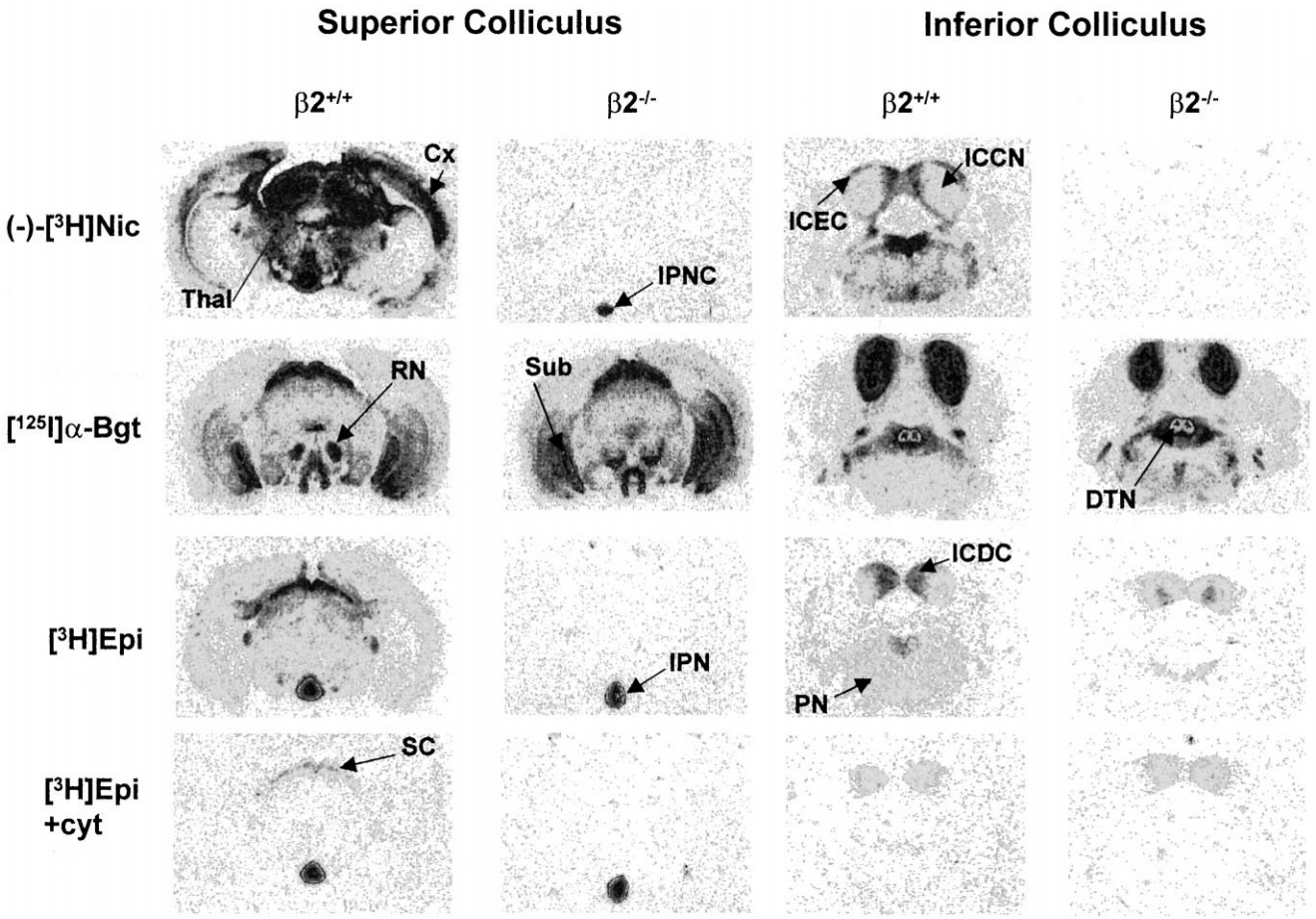

Fig. 1. Autoradiographic representation of (−)-[^{3}H]nicotine, [^{125}I]α-bungarotoxin, and [^{3}H]epibatidine (total, and with 50 nM cytisine) binding in wild-type and β2 nicotinic acetylcholine receptor subunit-null mouse brain. Sections (14 μm) were collected at the level of the superior and inferior colliculi, then incubated with 20 nM (−)-[^{3}H]nicotine (top row), 2 nM [^{125}I]α-bungarotoxin (second row), 500 pM [^{3}H]epibatidine alone (third row), or 500 pM [^{3}H]epibatidine + 50 nM cytisine (last row) as described in the Methods section. The panels are digital images of autoradiograms. The abbreviations used to identify brain regions are: Cx, cortex; DTN, dorsal tegmental nucleus; ICCN, inferior colliculus (central nucleus); ICDC, inferior colliculus (dorsal cortex); ICEC, inferior colliculus (external cortex); IPN, interpeduncular nucleus; IPNC, interpeduncular nucleus (caudal nucleus); PN, pontine nuclei; RN, red nucleus; SC, superior colliculus; Sub, subiculum; Thal, thalamus.

At the level of the inferior colliculus, (−)-[^{3}H]nicotine binding was largely restricted to the external cortex of the inferior colliculus, the pontine nuclei, and to the area surrounding the dorsal tegmental area, while [^{125}I]α-bungarotoxin labeling was particularly intense in the central nucleus and dorsal cortex of the inferior colliculus, and in the dorsal tegmental nucleus itself. At the level of the superior colliculus, [^{3}H]epibatidine binding was similar to that of (−)-[^{3}H]nicotine, but with a striking increase in binding in the dorsal cortex compared to the rest of the inferior colliculus. In these sections, cytisine-resistant [^{3}H]epibatidine binding was almost exclusively located in the dorsal cortex of the inferior colliculus.

Deletion of the nicotinic acetylcholine receptor β2 subunit had a dramatic effect on the expression of (−)-[^{3}H]nicotine binding, eliminating it in all regions studied, apart from the caudal subnucleus of the interpeduncular nucleus (where binding was greatly reduced). In contrast, β2 subunit deletion had no discernable effect on [^{125}I]α-bungarotoxin binding. Overall levels of [^{3}H]epibatidine binding were greatly reduced by β2 subunit deletion, but binding remained in the interpeduncular nucleus, central nucleus and dorsal cortex of the inferior colliculus, and a small subset of the pontine nuclei. Cytisine-resistant [^{3}H]epibatidine binding in the interpeduncular nucleus was unaffected by loss of β2 subunit expression, which also had little effect on cytisine-resistant [^{3}H]epibatidine binding in the inferior colliculus. In contrast, cytisine-resistant [^{3}H]epibatidine binding in the superficial layers of the superior colliculus and pontine nuclei was eliminated in the absence of the β2 subunit.

3.2. Membrane binding: low and high [^{3}H]epibatidine concentrations

As shown by Marks et al. (1999), [^{3}H]epibatidine binds to two classes of nicotinic sites: those with K_d values in

the picomolar range, and those with nanomolar affinity for the ligand. The effects of β2 genotype on both sets of binding sites are illustrated in Fig. 2.

As shown in Fig. 2 (top row), cytisine inhibited [^{3}H]epibatidine binding to mouse whole-brain membrane preparations in a biphasic manner. Labeling with 500 pM [^{3}H]epibatidine saturated the high-affinity binding sites, of which approximately 15–20% were cytisine-resistant (Marks et al., 1999). As predicted by the autoradiography experiments, loss of the β2 nicotinic acetylcholine receptor subunit reduced the number of whole-brain high-affinity [^{3}H]epibatidine binding sites by approximately 95%. In β2-heterozygous animals, high-affinity [^{3}H]epibatidine binding sites were reduced by approximately 50%, demonstrating a clear gene dosage effect. Cytisine-resistant [^{3}H]epibatidine binding sites (defined in the presence of 50 nM cytisine) were proportionately less affected by loss of β2 gene expression: heterozygous β2-null mutants retained approximately 75% of wild-type cytisine-resistant [^{3}H]epibatidine binding, while homozygous β2-null mutants expressed 5 fmol/mg protein of cytisine-resistant [^{3}H]epibatidine binding, or approximately 25% of that seen in wild-type animals. Whole-brain cytisine-sensitive [^{3}H]epibatidine binding (corresponding to (−)-[^{3}H]nicotine binding sites; Marks et al., 1998) fell to undetectable levels in the absence of β2 subunit expression. Thus, all

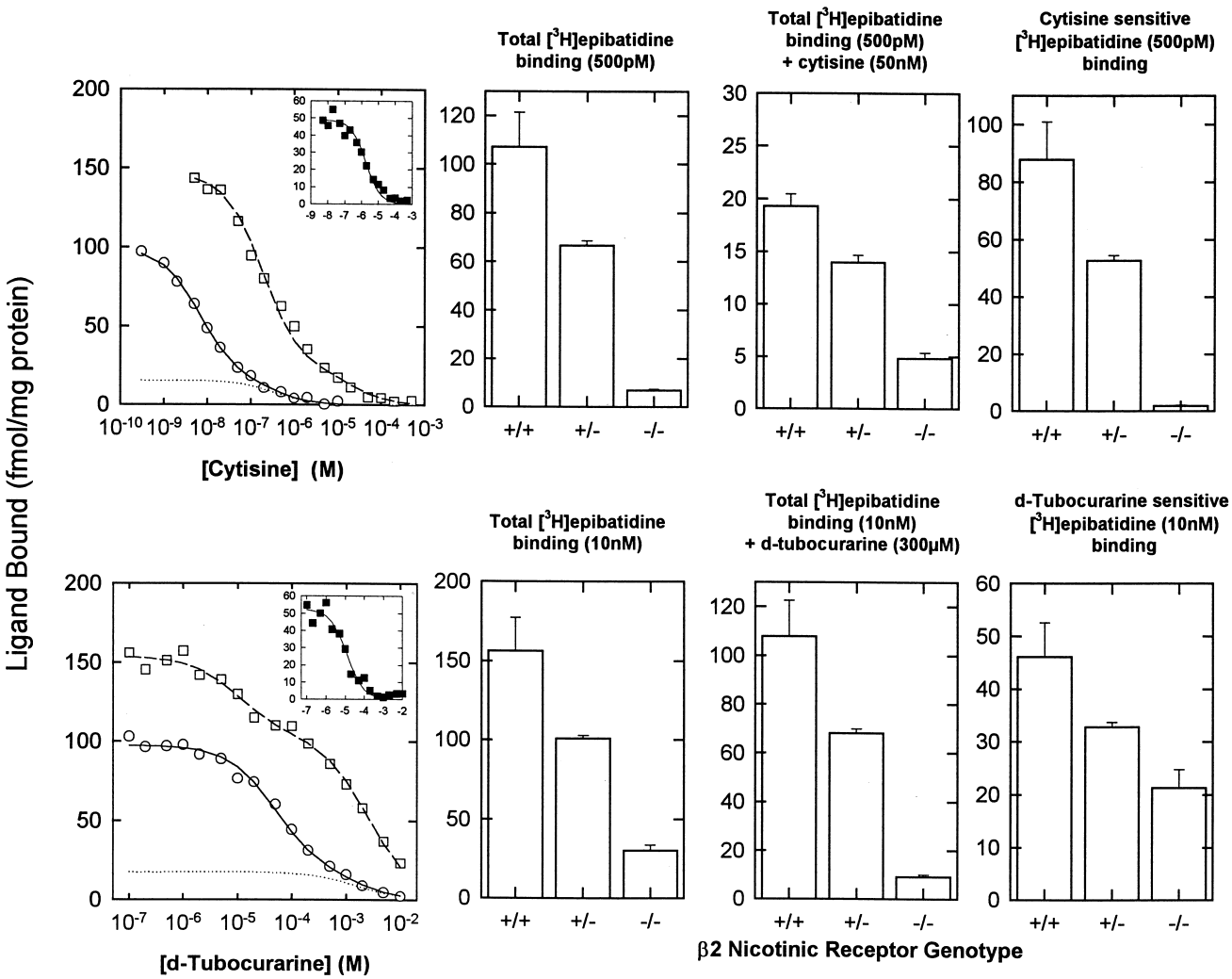

Fig. 2. [^{3}H]Epibatidine binding at low (500 pM) and high (10 nM) ligand concentrations: effect of β2 genotype. [^{3}H]Epibatidine binding to whole brain mouse particulate fractions was measured as described in the Methods section. The top left panel represents inhibition of [^{3}H]epibatidine binding by cytisine at low- (○) and high- (□) labeled ligand concentrations, while the bottom left panel displays inhibition by D-tubocurarine at the same labeled ligand concentrations. The lines represent two site Michaelis–Menten fits to the data. The inset panels show the difference in [^{3}H]epibatidine binding inhibition observed between assays using high and low concentrations, and represent calculated inhibition profiles for low-affinity [^{3}H]epibatidine binding. The remaining panels in the upper row show the effects of β2 genotype on total high-affinity [^{3}H]epibatidine binding, cytisine resistant high-affinity [^{3}H]epibatidine binding, and cytisine sensitive high-affinity [^{3}H]epibatidine binding. The remaining panels in the bottom row illustrate the effect of β2 genotype on total (low + high affinity) [^{3}H]epibatidine binding at 10 nM labeled ligand, binding of 10 nM [^{3}H]epibatidine + 300 μM D-tubocurarine (high-affinity [^{3}H]epibatidine binding only), and D-tubocurarine (300 μM) sensitive binding of 10 nM [^{3}H]epibatidine (high-affinity [^{3}H]epibatidine binding only). Each bar represents the mean ± SEM of at least four independent determinations.

whole-brain [^{3}H]epibatidine binding detectable in homozygous β2-null mice was cytisine resistant.

As shown in Fig. 2 (left column, insets), low-affinity [^{3}H]epibatidine binding sites (defined as the difference between sites detected using 500 pM and 10 nM [^{3}H]epibatidine; Marks et al., 1999) comprised approximately 50 fmol/mg protein in wild-type animals. Again, most [^{3}H]epibatidine binding at 10 nM ligand was dependent on β2 subunit expression: in the absence of β2 subunit expression, only 20 fmol/mg protein of sites were retained, from a wild-type population of 150 fmol/mg protein. Heterozygous β2-null mutants retained an intermediate amount of [^{3}H]epibatidine binding. High-affinity [^{3}H]epibatidine binding sites defined using 10 nM [^{3}H]epibatidine in the presence of 300 μM dTC (Marks et al., 1999) were indistinguishable from those defined with 500 pM [^{3}H]epibatidine. Low-affinity [^{3}H]epibatidine binding sites were considerably less sensitive to β2 genotype than high-affinity sites, with approximately 40% being retained in homozygous β2-null mutant animals. Again, a clear gene dosage effect was seen: heterozygous β2-null mutant animals expressed an intermediate density of low-affinity [^{3}H]epibatidine binding sites.

3.3. Synaptosomal efflux assays: inter-assay comparisons

In order to compare the pharmacological properties of the various nicotinic acetylcholine receptor activation assays developed in this laboratory, the EC_{50} and maximum efflux (E_{max}) values for a core group of nine nicotinic receptor agonists (acetylcholine, anatoxin-a, carbamylcholine, cytisine, epibatidine, methylcarbamylcholine, (−)-nicotine, (+)-nicotine, and tetramethylammonium) were determined in each assay. In some cases, other agonists were also assessed.

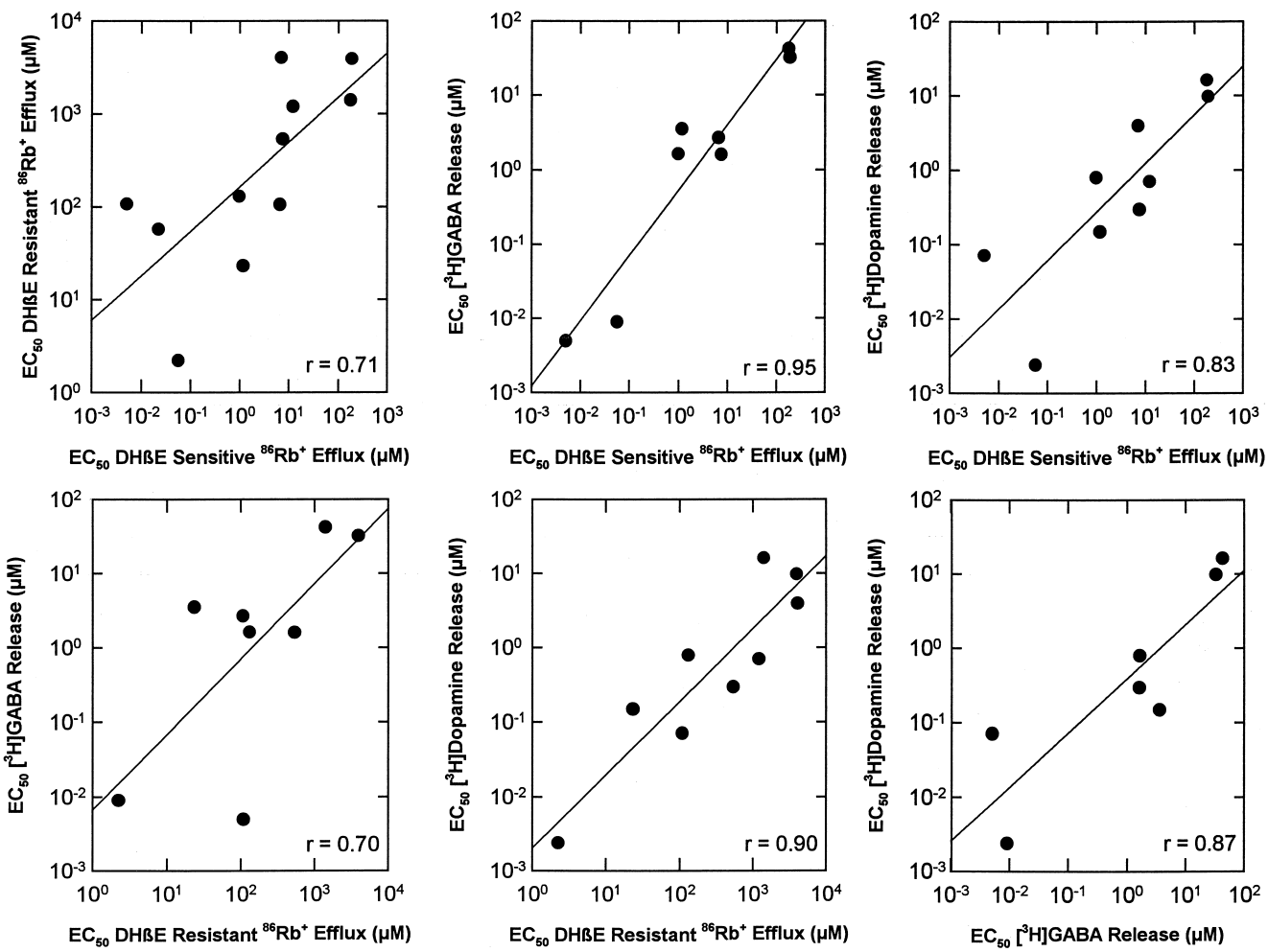

Fig. 3. Comparisons of agonist potencies in synaptosomal $^{86}Rb^+$-, [^{3}H]dopamine-, and [^{3}H]GABA-efflux assays. EC_{50} values were determined for a panel of nicotinic receptor agonists in the continuous flow monitoring $^{86}Rb^+$-efflux, [^{3}H]dopamine-, and [^{3}H]GABA-release synaptosomal nicotinic acetylcholine receptor activation assays, as described in the Materials and Methods section. Points represent the means of at least three independent determinations, error bars were omitted for clarity.

Pairwise comparisons of agonist potency are shown in Fig. 3. Dramatic differences in relative agonist potency between assays were not observed, as shown by the statistically significant correlations in EC_{50} values (the lowest r value measured was 0.70, the highest was 0.95, between the [^{3}H]GABA and DHβE-resistant $^{86}Rb^+$ efflux and the [^{3}H]GABA and DHβE-sensitive $^{86}Rb^+$ efflux assays, respectively). However, EC_{50} values at the DHβE-resistant response were typically two orders of magnitude higher than those measured in the other assays.

Larger differences were noted between assays in comparisons of relative agonist efficacies, as shown in Fig. 4. Agonist efficacies in [^{3}H]GABA and DHβE-sensitive $^{86}Rb^+$ efflux assays were highly correlated ($r = 0.91$), echoing the high correlation in agonist potencies between these two measures of nicotinic acetylcholine receptor activation. Each of the other pairs of assays showed noticeably lower correlation between agonist efficacies than were noted for agonist potencies, with the poorest match of agonist potencies observed between the [^{3}H]dopamine and DHβE-resistant $^{86}Rb^+$ efflux assays ($r = 0.12$).

3.4. Synaptosomal efflux assays: effect of β2 genotype

The effects of β2 genotype on each of the nicotinic acetylcholine receptor activation assays were studied, and the results are summarized in Fig. 5. Previous work identified the standard (fraction collecting) synaptosomal $^{86}Rb^+$ efflux response as being mediated by nicotinic acetylcholine receptors of the α4β2 subtype (Marks et al., 1996). As might be expected, loss of β2 subunit expression resulted in loss of standard $^{86}Rb^+$ efflux stimulated by 10 μM (−)-nicotine (1.55 ± 0.16% of tissue contents in wild type animals, 0.13 ± 0.03% in homozygous β2-null mutants). Although some loss of response was seen in heterozygous β2-null mutants, the majority of the response was retained (1.15 ± 0.06% of tissue contents, or 74% of wild-type activity). In contrast, the effect of β2 genotype on (−)-[^{3}H]nicotine binding, which measures α4β2 nicotinic acetylcholine receptor density, was more noticeable in heterozygous β2-null mutant animals than in the functional assay: whole-brain binding dropped to 24.4 ± 0.8 fmol/mg protein, or 55% of wild-type levels of 44.4 ± 7.0

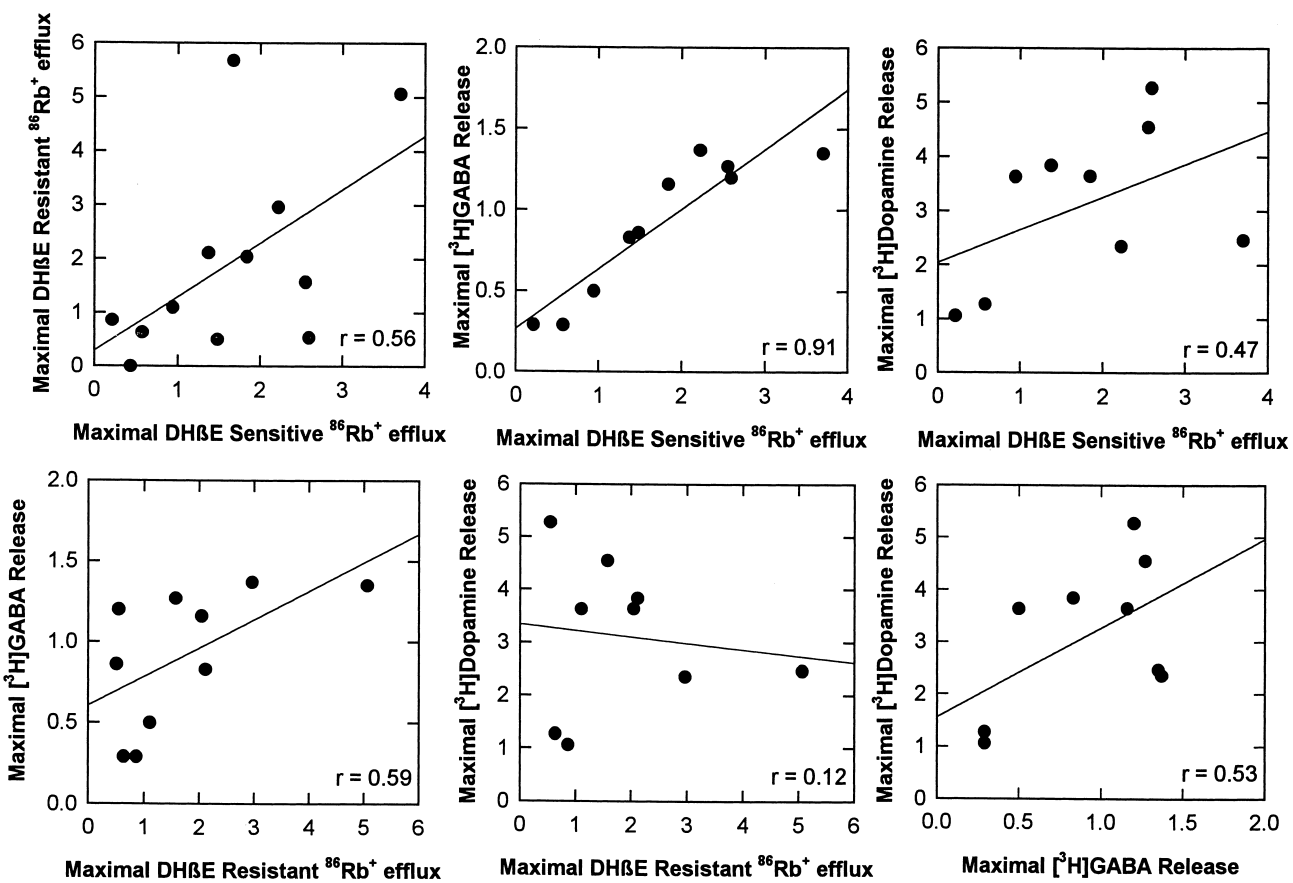

Fig. 4. Comparisons of agonist efficacies in synaptosomal $^{86}Rb^+$-, [^{3}H]dopamine-, and [^{3}H]GABA-efflux assays. Maximum activation elicited by a panel of nicotinic receptor agonists was measured in the continuous flow monitoring $^{86}Rb^+$-efflux, [^{3}H]dopamine-, and [^{3}H]GABA-release synaptosomal nicotinic acetylcholine receptor activation assays, as described in the Methods section. Points represent the means of at least three independent determinations, error bars were omitted for clarity.

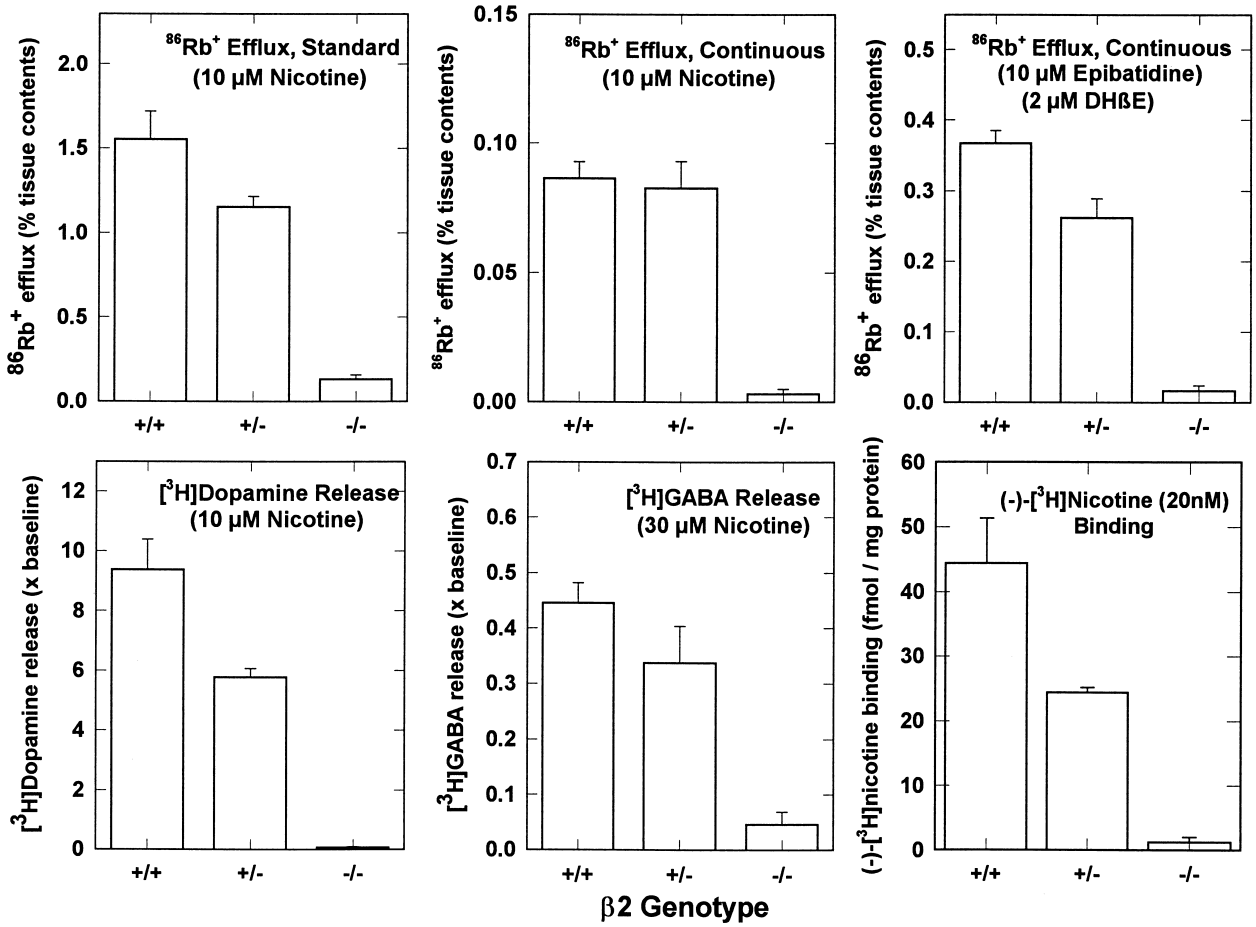

Fig. 5. Comparison of the effects of β2 nicotinic acetylcholine receptor subunit-null mutation on agonist induced synaptosomal $^{86}Rb^{+}$, [^{3}H]dopamine, and [^{3}H]GABA efflux. Synaptosomes were prepared from mice of each β2-null genotype (wild-type, heterozygous, and homozygous). The magnitude of $^{86}Rb^{+}$-efflux, [^{3}H]dopamine, and [^{3}H]GABA release evoked by a maximally stimulating dose of (−)-nicotine was determined for each genotype, in each assay. For comparison, the effect of β2 genotype on (−)-[^{3}H]nicotine binding to whole-brain membranes is also shown (bottom right panel). Values are the means ± SEM of at least three independent determinations.

fmol/mg protein. Whole-brain (−)-[^{3}H]nicotine binding was undetectable in homozygous β2-null mutants. The effects of β2-null mutation on each of the other functional responses were qualitatively similar to those measured on the standard $^{86}Rb^{+}$ efflux response, with almost complete elimination of nicotinic acetylcholine receptor mediated function in the homozygous β2-null mutants, and > 50% retention of function in the heterozygotes.

4. Discussion

The assays described in this study represent the results of an effort to develop and characterize a variety of nicotinic acetylcholine receptor-mediated binding and functional measures. The main motivation for this effort was to attempt to detect differences among the assays, pointing to underlying nicotinic acetylcholine receptor diversity. Success in this endeavor would be an important step towards identifying the expression and physiological roles of the potentially wide variety of mammalian neuronal nicotinic acetylcholine receptor subtypes.

In the autoradiography experiments, the pattern of [^{125}I]α-bungarotoxin (2 nM) binding was distinctively different from that of [^{3}H]epibatidine and (−)-[^{3}H]nicotine. This fits with the consensus that [^{125}I]α-bungarotoxin binding sites in mammalian brain differ from high-affinity agonist binding sites (Clarke et al., 1985; Pauly et al., 1989), and largely or entirely correspond to a single class of α7 containing nicotinic acetylcholine receptors. The lack of effect of β2 genotype on [^{125}I]α-bungarotoxin binding reinforces this identification. In contrast, (−)-[^{3}H]nicotine (20 nM) binding was heavily dependent upon the expression of the β2 nicotinic acetylcholine receptor subunit, as would be expected for a population thought to be almost exclusively composed of α4β2 subtype nicotinic acetylcholine receptors. A small population of high-affinity (−)-[^{3}H]nicotine binding sites was retained in the caudal nucleus of the interpeduncular nucleus in β2-null homozygous animals. This confirms the findings of Zoli et

al. (1998) and demonstrates that non-β2-containing nicotinic acetylcholine receptors can bind (−)-[^{3}H]nicotine with detectable affinity. As shown in Fig. 5, this novel population, while potentially important in the interpeduncular nucleus, represents a vanishingly small portion of the whole-brain (−)-[^{3}H]nicotine binding population.

Previous workers demonstrated that the majority of high-affinity [^{3}H]epibatidine binding occurs at (−)-[^{3}H]nicotine binding, α4β2 nicotinic acetylcholine receptors (Perry and Kellar, 1995; Marks et al., 1998). In addition to (−)-[^{3}H]nicotine binding sites, these workers also showed that [^{3}H]epibatidine binds with high affinity to a second population of nicotinic acetylcholine receptors, distinguished by a relatively low affinity for the nicotinic receptor agonist cytisine. As illustrated in Fig. 1, the differences in binding between (−)-[^{3}H]nicotine and [^{3}H]epibatidine can be explained by the presence of additional, cytisine-resistant [^{3}H]epibatidine binding sites. In agreement with Marks et al. (1998), the majority of high-affinity [^{3}H]epibatidine binding was abolished in animals lacking the β2 nicotinic acetylcholine receptor subunit. However, even in homozygous β2-null mutant animals, a small amount of high-affinity [^{3}H]epibatidine binding was detectable (Fig. 1). As shown in Fig. 1, some cytisine-resistant [^{3}H]epibatidine binding sites are retained in homozygous β2-null mutant mice. As noted by Marks et al. (1998), the pattern of cytisine-resistant [^{3}H]epibatidine binding site expression largely coincides with that of the α3 nicotinic acetylcholine receptor subunit mRNA, suggesting a role for this subunit in the cytisine-resistant [^{3}H]epibatidine binding sites. This hypothesis is supported by evidence from Parker et al. (1998) and Xiao et al. (1998), who show that heterologously expressed α3-containing nicotinic acetylcholine receptors have relatively low affinities for cytisine, but bind [^{3}H]epibatidine with high-affinity. Membrane binding experiments (Fig. 2) show that [^{3}H]epibatidine binding in homozygous β2-null mutant mice is exclusively cytisine-resistant. While cytisine-resistant [^{3}H]epibatidine binding sites in the interpeduncular nucleus and inferior colliculus are retained in the absence of β2 subunit expression, cytisine-resistant sites in the superficial layers of superior colliulus are lost in mice that do not express the β2 subunit. In homozygous β2-null mice, cytisine-resistant [^{3}H]epibatidine binding was found in regions expressing high levels of the β4 nicotinic acetylcholine receptor subunit (Dinelly-Miller and Patrick, 1992). Thus, it is possible that, in mouse brain, α3 and β4 subunits may combine to form cytisine-resistant [^{3}H]epibatidine binding nicotinic acetylcholine receptors.

In addition to labeling a variety of nicotinic acetylcholine receptor subtypes at low concentrations (500 pM), [^{3}H]epibatidine binds to lower affinity sites when used at concentrations (10 nM) similar to those employed for other ligands. As detailed in Fig. 2, these low-affinity sites are distinguished by a relatively high sensitivity to the antagonist D-tubocurarine. This identification is reinforced by the extremely close match between the amounts of high-affinity [^{3}H]epibatidine binding sites, and those detected using 10 nM [^{3}H]epibatidine + 300 μM D-tubocurarine (Fig. 2, Table 1). In a similar manner to their high-affinity counterparts, low-affinity [^{3}H]epibatidine binding sites may be divided into two groups, those that are lost in the absence of β2 subunit expression, and those that are retained. The identity of these low-affinity [^{3}H]epibatidine binding sites is not known, although it is possible that the β2 subunit-independent sites may correspond to α7 nicotinic acetylcholine receptors, which have a nanomolar affinity for [^{3}H]epibatidine (Gerzanich et al., 1995).

Thus, autoradiography and membrane binding studies demonstrate the existence of at least six nicotinic acetylcholine receptor subtypes: (1) [^{125}I]α-bungarotoxin binding, α7 containing nicotinic acetylcholine receptors; (2 and 3) high-affinity (−)-[^{3}H]nicotine binding sites dependent on, or independent of, β2 subunit expression; (4 and 5) β2 subunit-dependent and -independent cytisine-resistant [^{3}H]epibatidine binding sites; and (6) low-affinity [^{3}H]epibatidine binding sites that require β2 expression. In addition, if low-affinity [^{3}H]epibatidine binding sites, which are independent of β2 expression are not composed of α7 containing nicotinic acetylcholine receptors (see preceding paragraph), these may represent a seventh pharmacological subtype. The ligand binding studies illustrate an important point: the majority of the novel nicotinic acetylcholine receptor subtypes are concentrated in small, dispersed brain nuclei. Consequently, attempts to characterize these sites will be greatly assisted by concentrating on individual nuclei, rather than using whole-brain preparations. Further, subunit-null mutant mice may prove very useful in such attempts, by eliminating expression of nicotinic acetylcholine receptor subtypes (for instance, the α4β2), which mask the presence of the novel receptors.

As for the results of binding assay comparisons, activation pharmacologies vary between the synaptosomal release assays. Marks et al. (1999) demonstrated striking similarities between the properties of the standard (fraction collecting) $^{86}Rb^+$ efflux assay, and the DHβE-sensitive continuous flow $^{86}Rb^+$ efflux response, indicating that both were probably measures of activation at the same α4β2-subtype nicotinic acetylcholine receptor. This identification is reinforced by the abolition of both responses in β2-null homozygotes (Fig. 5). Interestingly, although (−)-[^{3}H]nicotine binding at α4β2-subtype nicotinic acetylcholine receptors is approximately halved in β2-null heterozygotes (Fig. 5), the effect on function in each of the assays is much less dramatic. This suggests that either a degree of functional compensation occurs in the heterozygous β2-null animals, whereby the remaining receptors are more functionally efficient, or wild-type animals express a substantial population of 'spare', or unused receptors.

As indicated by the high correlations in pairwise comparisons, no dramatic differences were observed in rank order of potency between functional assays, although it

should be noted that the absolute EC_{50} values of drugs for DHβE-resistant $^{86}Rb^+$ efflux were approximately 100-fold higher than for the other responses, indicating mediation by a different nicotinic acetylcholine receptor population. When agonist efficacies are considered, however, differences between the assays become much more apparent. For instance, the agonist potencies between the [^{3}H]dopamine release and DHβE-resistant $^{86}Rb^+$ efflux assays are highly correlated ($r = 0.90$), but when agonist efficacies are compared between assays this similarity disappears ($r = 0.12$). Only one pair of assays retained a high correlation between agonist potencies and efficacies ($r = 0.95$ and 0.91, respectively): [^{3}H]GABA release and DHβE-sensitive $^{86}Rb^+$ efflux. Together with the extremely similar absolute drug EC_{50} values between the two assays, this is strong evidence that whole-brain synaptosomal [^{3}H]GABA release is also mediated by α4β2 nicotinic acetylcholine receptors. Consequently, α4β2 nicotinic acetylcholine receptors may be assigned responsibility for at least the majority of nicotinically mediated [^{3}H]GABA release, and standard and DHβE-sensitive continuous flow $^{86}Rb^+$ efflux responses in whole-brain synaptosomal preparations. Conversely, [^{3}H]dopamine release and DHβE-resistant $^{86}Rb^+$ efflux are presumably evoked through another two, distinct nicotinic acetylcholine receptor subtypes. These additional nicotinic acetylcholine receptor subtypes are also dependent on expression of the β2 nicotinic acetylcholine receptor subunit. The results presented here show that the approach of comparing pharmacological properties across functional assays can be highly successful in illuminating underlying nicotinic acetylcholine receptor diversity. However, it is important to note that the common practice of comparing agonist potencies is relatively ineffectual in this regard. Given the generally poor subtype selectivity of existing nicotinic compounds, the full potential of this approach is only realized when other assay parameters (such as absolute potencies, and especially agonist efficacies) are considered simultaneously.

In conclusion, the studies described here have provided evidence for a wealth of pharmacologically distinct nicotinic acetylcholine receptor subtypes, responsible for both nicotinic activation and binding in mammalian brain. Some progress has been made in assigning particular measures to individual nicotinic acetylcholine receptor subtypes, but much work remains to be done in this regard. As the preliminary findings presented here for β2-null mutant mice demonstrate, the growing number of nicotinic acetylcholine receptor subunit mutants becoming available will provide invaluable assistance, as will the existence of a battery of reliable, pharmacologically distinct nicotinic assays. Interestingly, the β2-null mutant mice have so far proven to be of more use in discriminating between the nicotinic binding sites than the functional assays characterized to date (all of which are abolished by β2 subunit deletion). However, the ligand binding results indicate that individual brain nuclei may prove to be rich sources of novel nicotinic acetylcholine receptor subtypes, and would make excellent candidates for study using both ligand binding and functional approaches.

Acknowledgements

This work was supported by grants DA-03194 and DA-11156 from the National Institute on Drug Abuse. ACC is supported, in part, by Research Scientist Award DA-00197 from the National Institute on Drug Abuse.

References

Clarke, P.B.S., Schwartz, R.D., Paul, S.M., Pert, C.B., Pert, A., 1985. Nicotinic binding in rat brain: autoradiographic representation of [^{3}H]acetylcholine, [^{3}H]nicotine and [^{125}I]α-bungarotoxin. J. Neurosci. 5, 1307–1315.

Dinelly-Miller, K., Patrick, J., 1992. Gene transcripts for the nicotinic acetylcholine receptor subunit, β4, are distributed in multiple areas of the rat central nervous system. Mol. Brain Res. 16, 339–344.

Flores, C.M., Rogers, S.W., Pabreza, L.A., Wolfe, B.B., Kellar, K.J., 1992. A subtype of nicotinic cholinergic receptor in the brain is composed of α4 and β2 subunits and is upregulated by chronic nicotine treatment. Mol. Pharmacol. 41, 31–37.

Gerzanich, V., Peng, X., Wang, F., Wells, G., Anand, R., Fletcher, S., Lindstrom, J., 1995. Comparative pharmacology of epibatidine — a potent agonist for neuronal nicotinic acetylcholine-receptors. Mol. Pharmacol. 48, 774–782.

Grady, S.R., Grun, E.U., Marks, M.J., Collins, A.C., 1997. Pharmacological comparison of transient and persistent [^{3}H]dopamine release from mouse striatal synaptosomes and response to chronic L-nicotine treatment. J. Pharmacol. Exp. Ther. 282, 32–43.

Grady, S.R., Marks, M.J., Wonnacott, S., Collins, A.C., 1992. Characterization of [^{3}H]dopamine release from synaptosomes prepared from mouse striatum. J. Neurochem. 62, 848–856.

Lindstrom, J., Anand, R., Gerzanich, V., Peng, X., Wang, F., Wells, G., 1996. Structure and function of neuronal nicotinic acetylcholine receptors. Prog. Brain Res. 109, 125–137.

Lowry, A., Rosebrough, N.J., Farr, A.L., Randall, R.J., 1951. Protein measurement with the Folin phenol reagent. J. Biol. Chem. 193, 263–275.

Lu, Y., Grady, S., Marks, M.J., Picciotto, M., Changeux, J.-P., Collins, A.C., 1998. Pharmacological characterization of nicotinic receptor-stimulated GABA release from mouse brain synaptosomes. J. Pharmacol. Exp. Ther. 287, 648–657.

Marks, M.J., Farnham, D.A., Grady, S.R., Collins, A.C., 1993. Nicotinic receptor function determined by stimulation of rubidium efflux from mouse brain synaptosomes. J. Pharmacol. Exp. Ther. 264, 542–552.

Marks, M.J., Robinson, S.F., Collins, A.C., 1996. Nicotinic agonists differ in activation and desensitization of $^{86}Rb^+$ efflux from mouse thalamic synaptosomes. J. Pharmacol. Exp. Ther. 285, 377–386.

Marks, M.J., Smith, K.W., Collins, A.C., 1998. Differential agonist inhibition identifies multiple epibatidine binding sites in mouse brain. J. Pharmocol. Exp. Ther. 285, 377–386.

Marks, M.J., Whiteaker, P., Calcaterra, J., Stitzel, J.A., Bullock, A.E., Grady, S.R., Picciotto, M.R., Changeux, J.-P., Collins, A.C., 1999. Two pharmacologically distinct components of nicotinic receptor-mediated rubidium efflux in mouse brain require the β2 subunit. J. Pharmacol. Exp. Ther. 289, 1090–1103.

Marubio, L.M., Arroyo-Jimenez, M.M., Cordero-Erausquin, M., Léna,

C., Le Novère, N., Exaerde, A.K., Huchet, M., Damaj, M.I., Changeux, J.-P., 1999. Reduced antinociception in mice lacking nicotinic receptor subunits. Nature 287, 805–810.

Parker, M.J., Beck, A., Luetje, C.W., 1998. Neuronal nicotinic receptor β2 and β4 subunits confer large differences in agonist binding affinity. Mol. Pharmacol. 54, 1132–1139.

Pauly, J.R., Stitzel, J.A., Marks, M.J., Collins, A.C., 1989. An autoradiographic analysis of cholinergic receptors in mouse brain. Brain Res. Bull. 22, 453–459.

Perry, D.C., Kellar, K.J., 1995. [^{3}H]Epibatidine labels nicotinic receptors in rat brain: an autoradiographic study. J. Pharmacol. Exp. Ther. 275, 1030–1034.

Picciotto, M.R., Zoli, M., Lena, C., Bessis, A., Lallemand, Y., LeNovere, N., Vincent, P., Merlo-Pich, E., Brulet, P., Changeux, J.-P., 1995. Abnormal avoidance learning in mice lacking functional high-affinity nicotine receptor in mouse brain. Nature (London) 274, 65–67.

Schoepfer, R., Conroy, W.G., Whiting, P., Gore, M., Lindstrom, J., 1990. Brain α-bungarotoxin binding protein cDNAs and mAbs reveal subtypes of this branch of the ligand-gated ion channel gene superfamily. Neuron 5, 35–48.

Seguela, P., Wadiche, J., Dineley-Miller, K., Dani, J.A., Patrick, J.W., 1992. Molecular cloning, functional properties and distribution of rat brain α7: a nicotinic cation channel highly permeable to calcium. J. Neurosci. 13, 596–604.

Whiting, P., Lindstrom, J., 1987. Purification and characterization of nicotinic acetylcholine receptor from rat brain. Proc. Natl. Acad. Sci. U. S. A. 84, 595–599.

Wonnacott, S., 1997. Presynaptic nicotinic acetylcholine receptors. Trends Neurosci. 20, 92–98.

Xiao, Y., Meyer, E.L., Thompson, J.M., Surin, A., Wrobelowski, J., Kellar, K.J., 1998. Rat α3β/4 subtype of neuronal nicotinic acetylcholine receptor stably expressed in a transfected cell line: pharmacology of ligand binding and function. Mol. Pharmacol. 54, 322–333.

Zoli, M., Léna, C., Picciotto, M.R., Changeux, J.-P., 1998. Identification of four classes of brain nicotinic receptors using β2 mutant mice. J. Neurosci. 18, 4461–4472.